Soliton stability and collapse in the discrete nonpolynomial Schrödinger equation with dipole-dipole interactions

Goran Gligorić[1], Aleksandra Maluckov[2], Ljupčo Hadžievski[1], and Boris A. Malomed[3]
[1] *Vinča Institute of Nuclear Sciences, P.O. Box 522,11001 Belgrade, Serbia*
[2] *Faculty of Sciences and Mathematics, University of Niš, P.O. Box 224, 18001 Niš, Serbia*
[3] *Department of Physical Electronics, School of Electrical Engineering, Faculty of Engineering, Tel Aviv University, Tel Aviv 69978, Israel*

The stability and collapse of fundamental unstaggered bright solitons in the discrete Schrödinger equation with the nonpolynomial on-site nonlinearity, which models a nearly one-dimensional Bose-Einstein condensate trapped in a deep optical lattice, are studied in the presence of the long-range dipole-dipole (DD) interactions. The cases of both attractive and repulsive contact and DD interaction are considered. The results are summarized in the form of stability/collapse diagrams in the parametric space of the model, which demonstrate that the the attractive DD interactions stabilize the solitons and help to prevent the collapse. Mobility of the discrete solitons is briefly considered too.

PACS numbers: 03.75.Lm; 05.45.Yv

I. INTRODUCTION

It is well established that the mean-field description of Bose-Einstein condensates (BECs) trapped in a deep optical lattice can be reduced, starting from the one-dimensional (1D) Gross-Pitaevskii equation with the cubic nonlinearity, to the discrete nonlinear Schrödinger (DNLS) equation [1, 2]. However, while the DNLS equation with the cubic on-site nonlinearity readily predicts solitons [3], it cannot describe the dynamical collapse, which is often observed experimentally in the self-attractive BEC [4], [5].

In the general case, the reduction of the 3D Gross-Pitaevskii equation for the BEC trapped in a "cigar-shaped" configuration to the 1D form leads, instead of the "naive" cubic Schrödinger equation, to ones with a nonpolynomial nonlinearity [6, 8]. Such models are useful in various settings, making it possible to obtain results in a relatively simple form, which compare well to direct simulations of the underlying 3D equations [7]. In particular, the version of this model corresponding to the combination of the tight transverse trap and strong optical-lattice potential acting in the longitudinal direction takes the form of the discrete nonpolynomial Schrödinger equation (DNPSE), which was introduced recently [9]. An essential property of both the continual nonpolynomial equation and its discrete counterpart is that they make it possible to model the collapse.

A new variety of the BEC dynamics, dominated by long-range (nonlocal) interactions, occurs in dipolar condensates, which can be composed of magnetically polarized ^{52}Cr atoms, as demonstrated in a series of experimental works [10]. In particular, the dipole-dipole (DD) attraction in the condensate may give rise to a specific d-wave mode of the collapse [12]. On the other hand, the ^{52}Cr condensate can be efficiently stabilized against the collapse, adjusting the scattering length of the contact interaction by means of the Feshbach-resonance (FR) technique [11]. Another theoretically analyzed possibility is to create a condensate dominated by DD interactions between electric dipole moments induced in atoms by a strong external dc electric field [13]. A similar situation may be realized in BEC formed by dipolar molecules [14]. In particular, recent experimental work [15] has reported the creation of LiCs dipolar molecules in a mixed ultracold gas.

A possibility of making 2D solitons in dipolar condensates was predicted in several works. In particular, isotropic solitons [17] and vortices [18] may exist if the sign of the DD interaction is inverted by means of rapid rotation of the dipoles [16]. On the other hand, stable anisotropic solitons can be supported by the ordinary DD interaction, if the dipoles are polarized in the 2D plane [19]. Solitons supported by nonlocal interactions were also predicted and realized in optics, making use of the thermal nonlinearity [20].

A natural extension of the consideration of the dipolar BEC includes a strong optical lattice potential, which leads to the discrete model with the long-range DD interactions between lattice sites [21, 22]. In particular, 1D unstaggered solitons in this model with the cubic on-site nonlinearity were studied in Ref. [21]. It was shown that the DD interactions might enhance the solitons' stability. This conclusion suggests a possibility of suppressing the collapse by means of the long-range DD forces, but the study of the collapse is not possible in the discrete system with the cubic nonlinearity. The objective of the present work is to introduce the DD interaction into DNPSE model and analyze the effects of the long-range interactions between dipoles localized at site of the discrete lattice on the soliton's collapse in the sufficiently dense self-attractive condensate trapped in the deep optical lattice potential. We here focus on unstaggered solitons, leaving the consideration of staggered ones for another work.

The paper is structured as follows. The discrete model including the on-site nonpolynomial nonlinearity and long-range DD interactions is formulated in Section II.

Results for on-site and inter-site solitons, including the study of their stability, and the possibility of the collapse onset, are presented in Section III. The mobility of discrete solitons in the DNPSE model is also briefly considered in Section III. The paper is concluded by Section IV.

II. THE MODEL

Adding the long-range DD interaction to the scaled nonpolynomial Schrödinger equation (in its continual form [6, 7]) leads to the following 1D equation:

$$i\frac{\partial F}{\partial t} = \left[-\frac{1}{2}\frac{\partial^2}{\partial z^2} - V_0\cos(2qz) + \frac{1-(3/2)\aleph|F|^2}{\sqrt{1-\aleph|F|^2}}\right]F + GF(z)\int_{-\infty}^{+\infty}\frac{|F(z')|^2}{|z-z'|^3}dz'. \quad (1)$$

Here, V_0 and π/q are the strength and period of the longitudinal optical lattice potential, $F(z,t) \equiv \sqrt{|\gamma|}f(z,t)$, where f is the 1D mean-field wave function subject to normalization $\int_{-\infty}^{+\infty}|f(z,t)|^2\,dz = 1$, and $\gamma = -2Na_s\sqrt{m\omega_\perp/\hbar}$ is the effective strength of the local interaction, with N the total number of atoms in the condensate, a_s the scattering length of atomic collisions ($a_s<0$ corresponds to the attraction), m the atom mass, and $\omega_\perp$ the transverse trapping frequency [6]. Further, $\aleph \equiv \mathrm{sgn}(a_s)$ is the sign of the local interaction, and $G = g\left(1-3\cos^2\theta\right)$ is the coefficient which defines the ratio of the DD and contact interactions, where g is a positive coefficient and θ the angle between the z axis and the orientation of the dipoles. One obvious case of interest in the 1D geometry corresponds to the dipoles polarized along the z axis, i.e., $\theta = 0$ and $G = -2g$, when the long-range interaction is *attractive*. Another interesting case corresponds to the orientation of the dipoles perpendicular to the z axis ($\theta = \pi/2$, i.e. $G = g$), which implies the repulsive DD interaction.

Assuming a sufficiently deep optical lattice potential, and approximating the wave function by a superposition of localized Wannier modes, similar to how it was done in Refs. [9] and [21], one can derive the discrete version of Eq. (1), i.e., the DNPSE with the DD term:

$$i\frac{\partial F_n}{\partial t} = -C\left(F_{n+1}+F_{n-1}-2F_n\right) + \frac{1-(3/2)\aleph|F_n|^2}{\sqrt{1-\aleph|F_n|^2}}F_n - \Gamma\sum_{n'\neq n}\frac{|F_{n'}|^2}{|n-n'|^3}F_n, \quad (2)$$

where the linear-coupling C and the ratio between DD and contact interaction coefficients $\Gamma = G/|\gamma|$, are defined as in Ref. [21] ($\Gamma>0$ for attractive and $\Gamma<0$ for the repulsive DD interactions). Two dynamical quantities are conserved by Eq. (2), *viz.*, norm $P = \sum_n |F_n|^2$ and Hamiltonian

$$H = \sum_n\left[C|F_n - F_{n+1}|^2 + \sqrt{1-\aleph|F_n|^2}\,|F_n|^2 - \Gamma\sum_{n\neq n'}\frac{|F_{n'}|^2|F_n|^2}{|n-n'|^3}\right]. \quad (3)$$

Note that the *staggering transformation*, $F_n \equiv (-1)^n\exp(-4iCt)\tilde{F}_n$, can be used to change the sign of C if it is negative, but this transformation cannot be used to invert the signs of nonlinearity coefficients in Eq. (2).

Experimentally adjustable parameters are the relative strength of the DD/contact interactions, Γ, and the norm of stationary wave function, P. The latter may be expressed in terms of the total number of atoms in the condensate, N [9, 21]: $P \sim N|a_s|\sqrt{m\omega_\perp/\hbar}$. In particular, $a_s \approx 5$ nm for ^{52}Cr atoms (far from the FR); assuming the transverse-confinement width to be $(\sqrt{m\omega_\perp/\hbar})^{-1} \sim 5$ μm, we conclude that $P\sim 1$ may correspond to ~ 1000 atoms in the condensate. A typical value of the relative interaction strength, if estimated as the ratio of the effective scattering lengths corresponding to the DD and contact interactions in the ^{52}Cr condensate, without the use of the FR technique, is $|\Gamma| \simeq 0.15$ [11]. Actually, Γ can be made both positive and negative, and its absolute value may be altered within broad limits by means of the FR [10]. In particular, $|\Gamma|$ can be given very large values in the experimentally possible situation when the strength of the contact interactions is almost nullified with the help of the FR [11].

Stationary solutions to Eq. (2), with chemical potential μ, are sought for as $F_n = u_n\exp(-i\mu t)$, with real discrete function u_n satisfying a stationary equation,

$$\mu u_n = -C\left(u_{n+1}+u_{n-1}-2u_n\right) + \frac{1-(3/2)\aleph u_n^2}{\sqrt{1-\aleph u_n^2}}u_n - \Gamma u_n\sum_{n'\neq n}\frac{u_{n'}^2}{|n-n'|^2}. \quad (4)$$

In the case of the attractive contact interaction ($\aleph = +1$), u_n^2 cannot exceed the maximum value, $\left(u_n^2\right)_{\max} = 1$, as seen from Eq. (4). In fact, the presence of the singularity in Eq. (2) at $|F_n|^2 = 1$ makes it possible to study the onset of collapse in the framework of this equation [9].

Stationary equation (4) was numerically solved by an algorithm based on the modified Powell minimization method [9, 21]. Initial *ansätze* used to construct on-site and inter-site-centered discrete solitons were taken, respectively, as $\left\{u_n^{(0)}\right\} = (..., 0, A, 0, ...)$ and $(..., 0, A, A, 0, ...)$, where A is a real constant obtained from Eq. (4) in the corresponding approximation.

Results reported below were obtained in the lattice composed of 101 or 100 sites, for the on-site and inter-site configurations, respectively. It was checked that the results do not alter if a larger lattice had been used.

III. RESULTS AND DISCUSSION

A. The case of the attractive contact interaction

Families of fundamental unstaggered solitons of on-site and inter-site types for the local attraction ($\aleph = +1$) and either sign of the DD interaction were obtained from the numerical solution of Eq. (4). In contrast to the 1D discrete model with the cubic on-site nonlinearity, where bright unstaggered solitons exist only for sufficiently weak repulsive DD interaction [21], in the present model solitons can be also found if the repulsive DD interaction is strong. The solitons were categorized as stable ones if they met two conditions: the slope (*Vakhitov-Kolokolov*) criterion, according to which the slope of the $P(\mu)$ dependence must be negative (or may be very close to zero, see below), $dP/d\mu \leq 0$, and, simultaneously, the spectral condition, according to which the corresponding eigenvalues, found from linearized equations for small perturbations, must not have a positive real part [21, 23].

In order to draw general conclusions about the influence of the DD interaction on the solitons, the analysis is presented below for two different values of the lattice coupling constant C, *viz.*, $C = 0.8$ and $C = 0.2$. These cases correspond, respectively, to the proximity to the continuum limit, and to a strongly discrete system.

1. The quasi-continual model ($C = 0.8$)

A global characteristic of soliton families is the $P(\mu)$ dependence, i.e., the scaled norm as a function of the chemical potential. For $C = 0.8$ and four different values of DD parameter Γ, the $P(\mu)$ curves are displayed in Fig. 1. In the absence of the DD interaction, $\Gamma = 0$, two subfamilies of on-site solitons are found, one (which occupies a narrow interval of μ) obeying the slope criterion, and the other one violating it, in a broad interval. With the increase of the strength of the attractive DD interactions ($\Gamma = 5$), the region where the slope condition is met spreads out, and, when the DD interaction is dominant ($\Gamma = 12$), the condition is satisfied for all on-site solitons. On the other hand, the slope condition is fulfilled for all inter-site solitons, regardless of the value of Γ. It is worthy to note that the difference between the $P(\mu)$ curves for the on-site and inter-site solitons vanishes as the attractive DD interaction strengthens.

In the case of the repulsive DD interaction, the $P(\mu)$ curves for on-site and inter-site solitons are completely separated, see Fig. 1(d). Actually, the slope of $P(\mu)$ curves for both on-site and inter-site solitons tends to be very small in this case, which makes the application of the slope criterion doubtful. In these areas, the solitons feature the amplitude close to the upper limit admitted by the model, $u^2_{\max} = 1$, and a very small width, corresponding to a situation when nearly all atoms are collected in a single well of the underlying potential lattice.

The spectral stability was examined by linearizing Eq. (2) for small perturbations δF_n around the soliton, and finding the respective eigenvalues in a numerical form. The results of the stability analysis for the on-site solitons, with $C = 0.8$, are summarized in Fig. 2, in the form of the stability diagram in the plane of (μ, Γ), where contours of constant norm P for the on-site solitons are included too. The collapse condition, $u^2_{\max} = 1$, is attained at the black solid line, which is, simultaneously, a stability border. In direct simulations, the on-site solitons which are predicted to be stable survived as long as the simulations ran [Fig. 3(a)], while the solitons classified as unstable ones suffered the collapse (destruction of the solution after attaining the level of $u^2_{\max} = 1$) in a finite time.

On the other hand, all inter-site solitons are unstable, as the spectrum of eigenvalues for small perturbations around them always contains real eigenvalues. However, unstable inter-site solitons which have stable on-site counterparts with the same norm avoid the collapse, evolving into robust breathers oscillating around the corresponding stable on-site solitons, as shown in Fig. 3(b). Unstable inter-site solitons do collapse if no stable on-site soliton with the same norm can be found, see Fig. 3(c). Therefore, the border line for the collapse of the inter-site solitons coincides with the stability border for on-site solitons in Fig. 2.

For the repulsive DD interaction, the spectral stability condition for all inter-site solitons does not hold either. Because, in this case, curves $P(\mu)$ for the inter-site and on-site solitons are strongly separated [Fig.1(d)], unstable inter-site solitons do not find stable on-site counterparts with the same norm, therefore they suffer the collapse. As for the on-site solitons, there exists a region where the spectral stability condition holds for them. This region expands as the repulsive DD interaction gets stronger, although the respective curve $P(\mu)$ becomes almost horizontal, and the slope condition cannot be accurately verified. Direct numerical simulations confirm the predictions of the stability analysis for the on-site solitons in this case too.

2. The strongly discrete model ($C = 0.2$)

In this case, the slope condition is satisfied for all on-site solitons in the absence of the DD interaction ($\Gamma = 0$), see Fig. 4(a). As the strength of the attractive DD interaction grows, a pair of subfamilies emerge, the slope-stable and unstable ones, the respective $P(\mu)$ curves being similar to those observed in the case of the strong coupling, $C = 0.8$ [Fig. 4(b)]. Eventually, when the attractive DD interaction becomes dominant, the region

where the slope condition is satisfied spreads over the entire parameter space, as seen in Fig. 4(c).

In the model with $C = 0.2$, all inter-site solitons again satisfy the slope condition. With the strengthening of the DD interaction, the separation between the $P(\mu)$ curves for the on-site branch, which satisfies the slope condition, and its inter-site counterpart vanishes. On the other hand, in the case of the repulsive DD interaction, the corresponding $P(\mu)$ curves for on-site and inter-site soliton families are strongly separated, see Fig. 4(d).

Results of the stability analysis for the on-site solitons are summarized in the stability diagram displayed in Fig. 5(a) in parametric space (Γ, μ). Unlike the case of $C = 0.8$, cf. Fig. 2, in the present case there appears a region where the spectral stability condition is violated for on-site solitons as the DD interaction grows stronger, as well as a region where the stability condition holds for inter-site solitons. These regions disappear again with the further growth of Γ. Also in contrast to the case of $C = 0.8$, the line at which the collapse is attained in the family of on-site solitons *does not* coincide with the border between stable and unstable parts of the family. Rather, the collapse line passes trough the unstable region where the spectral-stability condition does not hold, see Fig. 5(a). Direct simulations demonstrate that unstable on-site solitons which have stable inter-site counterparts with the equal norm evolve into breathers oscillating around the stable counterparts. On the other hand, if unstable on-site solitons cannot find stable inter-site counterparts with the same (or close) value of the norm, they undergo the collapse. In fact, the existence of the two different scenarios of the instability development – the formation of the breather and collapse – explains the above-mentioned fact that the collapse line does not coincide with the instability border. In the present case too, direct simulations corroborate the stability of those solitons which do not have unstable eigenvalues.

Extending the above-mentioned trend, unstable inter-site solitons which have stable on-site counterparts with the same norm evolve into persistent breathers, while those unstable solitons that are devoid of stable equal-norm counterparts suffer the collapse. Accordingly, the line at which the collapse is attained does not coincide with the instability border, as seen in Fig. 5(b). It is worthy to note the existence of a stability region for inter-site solitons in Fig. 5(b) which is adjacent to the collapse line. In the latter case, the stable inter-site solitons do not have on-site counterparts with the same value of the norm.

For the repulsive DD interactions, the spectral stability condition always holds for on-site solitons and does not hold for inter-site modes, similar to the case of $C = 0.8$. Again, in some part of the parameter space, the corresponding $P(\mu)$ curves for the on-site solitons are nearly horizontal lines with zero slope, being completely separated from the $P(\mu)$ line for the inter-site modes. Direct simulations demonstrate that the on-site solitons are indeed stable in this case, while the unstable inter-site solitons undergo the collapse.

B. The case of repulsive contact interactions

If the local interaction is repulsive, the existence of the unstaggered solitons may only be supported by the attractive DD interaction. In the model with the self-repulsive cubic on-site nonlinearity, unstaggered solitons were found only when the relative strength of the attractive DD interaction was large enough, $\Gamma \geq 0.4$ [21]. In the present model, unstaggered solitons (with large amplitudes) are obtained for smaller values of Γ as well. Nevertheless, general results obtained in the present model for the case of the local repulsion are not drastically different from those reported in the model with the cubic on-site nonlinearity in Ref. [21]. In particular, differences between $P(\mu)$ curves for on-site and inter-site solitons are small at all values of μ, the slope condition is always satisfied for both types of the solitons, and there is an exchange between regions where the spectral stability condition is fulfilled for on-site and inter-site solitons. Further, unstable solitons evolve into breathers oscillating around their stable counterparts. The similarity of these results for discrete solitons in the present DNPSE model and its cubic counterpart is not surprising, as in the case of the local repulsion (unlike attraction) there is no dramatic difference between the nonpolynomial and cubic nonlinearities, therefore the competition of the local term of either type (nonpolynomial or cubic) with the DD attraction gives rise to similar solitary modes.

C. Moving discrete solitons

Finally, we briefly summarize results concerning mobility of localized modes, with respect to the concept of the Peierls-Nabarro barrier [24]. To this end, we follow the lines of the analysis developed in Refs. [9] and [21]. Examination of the mobility has shown that the Peierls-Nabarro barrier in the DNPSE model depends on the strength of the DD interaction in the same way as it was in the discrete model with the cubic on-site nonlinearity. Namely, in the case of the local attraction, the repulsive or attractive DD interaction decreases or increases, respectively, a region in plane (P, μ) where mobile localized modes can be found. On the other hand, in the case of the contact repulsion, all localized modes can be set in motion by an initial kick, regardless of the value of DD coefficient Γ. In all cases when mobile discrete solitons exist, the vanishing of the Peierls-Nabarro barrier coincides with the disappearance of the separation between $P(\mu)$ curves for the on-site and inter-site soliton families, cf. Refs. [9, 21].

IV. CONCLUSION

The purpose of this work was to achieve a better understanding on the influence of the long-range DD (dipole-dipole) interactions on the stability and collapse of localized nonlinear modes in the cigar-shaped Bose-Einstein condensate trapped in a deep optical-lattice potential. To this end, we have introduced the model based on the one-dimensional DNPSE (discrete nonpolynomial Schrödinger equation), which includes the contact (on-site) and DD nonlinear terms. Both attractive and repulsive signs of the contact and DD interactions were considered. The main conclusion is that the presence of the attractive DD interaction enhances the soliton's stability and helps to prevent the collapse. Our analysis was limited to unstaggered solitons, the consideration of staggered localized modes being a subject of a separate work.

G.G., A.M. and Lj.H. acknowledge support from the Ministry of Science, Serbia (through project 141034).

[1] A. Trombettoni and A. Smerzi, Phys. Rev. Lett. **86**, 2353 (2001); F. Kh. Abdullaev, B. B. Baizakov, S. A. Darmanyan, V. V. Konotop, and M. Salerno, Phys. Rev. A **64**, 043606 (2001); G. L. Alfimov, P. G. Kevrekidis, V. V. Konotop, and M. Salerno, Phys. Rev. E **66**, 046608 (2002); R. Carretero-González, K. Promislow, Phys. Rev. A **66,** 033610 (2002); N. K. Efremidis and D. N. Christodoulides, *ibid.* **67**, 063608 (2003).

[2] M. A. Porter, R. Carretero-González, P. G. Kevrekidis, and B. A. Malomed, Chaos **15**, 015115 (2005).

[3] P. G. Kevrekidis , K. O. Rasmussen and A. R. Bishop, Int. J. Mod. Phys. B **15**, 2833 (2001).

[4] K. E. Strecker, G. B. Partridge, A. G. Truscott and R. G. Hulet, Nature **417**, 150 (2002); see also K. E. Strecker, G. B. Partridge, A. G. Truscott, and R. G. Hulet, New J. Phys. **5**, 73 (2003).

[5] S. L. Cornish, S. T. Thompson and C. E. Wieman, Phys. Rev. Lett. **96**, 170401 (2006).

[6] L. Salasnich, Laser Phys. **12**, 198 (2002); L. Salasnich, A. Parola, and L. Reatto, Phys. Rev. A **65**, 043614 (2002); *ibid.* **66**, 043603 (2002).

[7] L. Salasnich, A. Parola, and L. Reatto, Phys. Rev. A **66**, 043603 (2002); L. Salasnich, Phys. Rev. A **70**, 053617 (2004);
L. Salasnich and B. A. Malomed, Phys. Rev. A **74**, 053610 (2006); L. Salasnich, A. Cetoli, B. A. Malomed, and F. Toigo, *ibid.* **75**, 033622 (2007); L. Salasnich, A. Cetoli, B. A. Malomed, F. Toigo, and L. Reatto, *ibid.* **76**, 013623 (2007); L. Salasnich, B. A. Malomed, and F. Toigo, *ibid.* **76**, 063614 (2007); **77**, 035601 (2008).

[8] A. M. Mateo and V. Delgado, Phys. Rev. Lett. **97**, 180409 (2006); A. Muñoz Mateo and V. Delgado, Phys. Rev. A 77, 013617 (2008).

[9] A. Maluckov, Lj. Hadžievski, B. A. Malomed, L. Salasnich, Phys. Rev. A **78**, 013616 (2008).

[10] A. Griesmaier, J. Werner, S. Hensler, J. Stuhler, and T. Pfau., Phys. Rev. Lett. **94**, 160401 (2005); J. Stuhler, A. Griesmaier, T. Koch, M. Fattori, T. Pfau, S. Giovanazzi, P. Pedri, and L. Santos, *ibid.* **95**, 150406 (2005); J. Werner, A. Griesmaier, S. Hensler, J. Stuhler, and T. Pfau, *ibid.* **94**, 183201 (2005); A. Griesmaier, J. Stuhler, T. Koch, M. Fattori, T. Pfau, and S. Giovanazzi, *ibid.* **97**, 250402 (2006); T. Lahaye, T. Koch, B. Fröhlich, M. Fattori, J. Metz, A. Griesmaier, S. Giovanazzi, and T. Pfau, Nature (London) **448**, 672 (2007).

[11] T. Koch, T. Lahaye, J. Metz, B. Fröhlich, A. Griesmaier, T. Pfau, Nature Physics **4**, 218 (2008).

[12] T. Lahaye, J. Metz, B. Froehlich, T. Koch, M. Meister, A. Griesmaier, T. Pfau, H. Saito, Y. Kawaguchi, and M. Ueda, Phys. Rev. Lett. **101**, 080401 (2008).

[13] M. Marinescu and L. You, Phys. Rev. Lett. **81**, 4596 (1998); S. Giovanazzi, D. O'Dell, and G. Kurizki, Phys. Rev. Lett. **88**, 130402 (2002); I. E. Mazets, D. H. J. O'Dell, G. Kurizki, N. Davidson, and W. P. Schleich, J. Phys. B 37, S155 (2004).

[14] J. Sage, S. Sainis, T. Bergeman, and D. DeMille, Phys. Rev. Lett. **94**, 203001 (2005); C. Ospelkaus, L. Humbert, P. Ernst, K. Sengstock, and K. Bongs, *ibid.* **97**, 120402 (2006); T. Köhler, K. Góral, and P. S. Julienne, Rev. Mod. Phys. **78**, 1311 (2006).

[15] J. Deiglmayr, A. Grochola, M. Repp, K. Mörtlbauer, C. Glück, J. Lange, O. Dulieu, R. Wester, and M. Weidemüller, Phys. Rev. Lett. **101**, 133004 (2008).

[16] S. Giovanazzi, A. Görlitz, and T. Pfau, Phys. Rev. Lett. **89**, 130401 (2002); A. Micheli, G. Pupillo, H. P. Büchler, and P. Zoller, Phys. Rev. A **76**, 043604 (2007).

[17] P. Pedri and L. Santos, Phys. Rev. Lett. **95**, 200404 (2005); R. Nath, P. Pedri, and L. Santos, Phys. Rev. A **76**, 013606 (2007).

[18] I. Tikhonenkov, B.A. Malomed, and A. Vardi. Vortex solitons in dipolar Bose-Einstein condensates. Phys. Rev. A **78**, 043614 (2008).

[19] I. Tikhonenkov, B. Malomed, and A. Vardi, Phys. Rev. Lett. **100**, 090406 (2008).

[20] C. Rotschild, O. Cohen, O. Manela, and M. Segev, Phys. Rev. Lett. **95**, 213904 (2005); D. Briedis, D. E. Petersen, D. Edmundson, W. Królikowski, and O. Bang, Opt. Exp. **13**, 435 (2005).

[21] G. Gligorić, A. Maluckov, Lj. Hadžievski, B. A. Malomed, Phys. Rev. A **78**, 063615 (2008).

[22] M. Klawunn and L. Santos, arXiv: 0812.3543.

[23] Y. Sivan, B. Ilan, G. Fibich, Phys. Rev. E **78**, 046602, (2008)

[24] Yu. S. Kivshar and D. K. Campbell, Phys. Rev. E **48**, 3077 (1993); Lj. Hadžievski, A**.** Maluckov, M. Stepić, and D. Kip, Phys. Rev. Lett. **93**, 033901 (2004); Z. Xu, Y. Kartashov, and L. Torner, Phys. Rev. Lett. **95**, 113901 (2005).

Figures

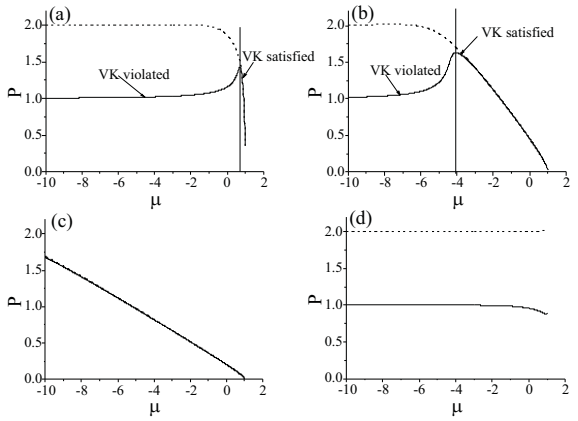

FIG. 1: The $P(\mu)$ (norm versus chemical potential) dependencies for families of on- and inter-site unstaggered solitons (the solid and dashed lines, respectively) in the case of the attractive contact interaction, for $C = 0.8$ and relative strength of the DD interaction $\Gamma = 0$ (a), 5 (b), 12 (c), and -5 (d).

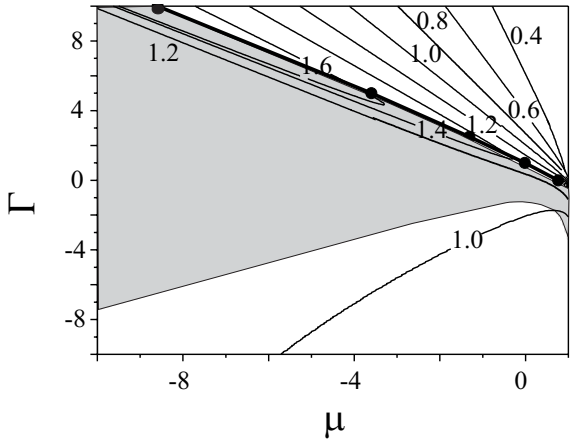

FIG. 2: The stability/collapse diagram for on-site solitons, as determined by the stability analysis performed for $C = 0.8$. The gray and white areas are occupied by unstable and stable solitons, respectively. The soliton norm keeps constant values along thin contour lines, as indicated in the figure. The chain of bold dots connected by the black line shows a curve along which the collapse is attained.

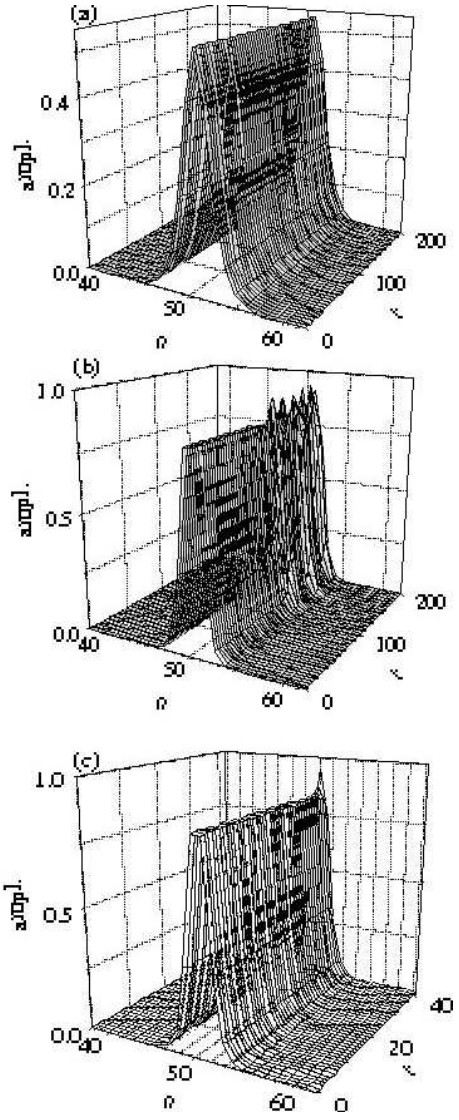

FIG. 3: (a) An example of a stable on-site soliton. (b,c) Development of the instability of inter-site solitons: (b) the case when a stable on-site soliton exists whose norm is equal to that of the unstable inter-site sooliton. In this situation, the unstable soliton evolves into a breather oscillating around the stable on-site soliton. (c) The case without the stable on-site counterpart with the equal norm. In the latter case, the unstable soliton collapses.

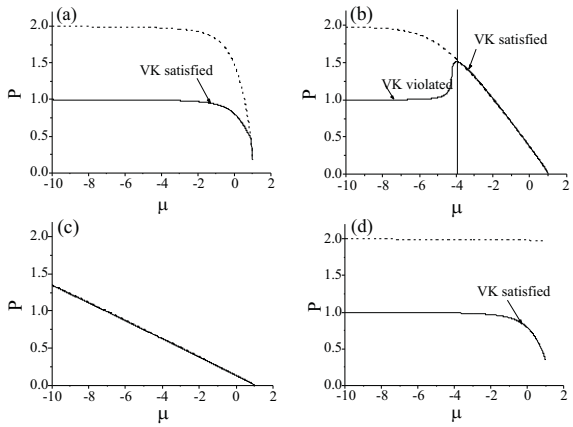

FIG. 4: $P(\mu)$ dependencies for families of on- and inter-site (solid and dashed lines, respectively) unstaggered solitons in the strongly discrete model ($C = 0.2$) with the attractive contact interaction. The relative strength of the DD interaction is $\Gamma = 0$ (a), 5 (b), 15 (c), and -5 (d).

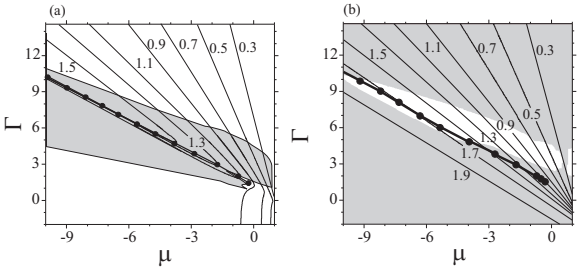

FIG. 5: The stability/collapse diagram for (a) on-site (a) and inter-site (b) unstaggered solitons in the strongly discrete version of the model, with $C = 0.2$. The notation has the same meaning as in Fig. 2.